Available online at www.sciencedirect.com

SCIENCE DIRECT

Toxicology and Applied Pharmacology 202 (2005) 84–98

Toxicology and Applied Pharmacology

www.elsevier.com/locate/ytaap

The monofunctional alkylating agent *N*-methyl-*N*′-nitro-*N*-nitrosoguanidine triggers apoptosis through p53-dependent and -independent pathways

Wan-Ju Kim[1], Dillon I. Beardsley[1], Aaron W. Adamson[2], Kevin D. Brown*

Department of Biochemistry and Molecular Biology, and the Stanley S. Scott Cancer Center, LSU Health Sciences Center, New Orleans, LA 70112, USA

Received 25 November 2003; accepted 10 June 2004
Available online 27 October 2004

Abstract

One of the cellular responses to DNA damaging events is the activation of programmed cell death, also known as apoptosis. Apoptosis is an important process in limiting tumorigenesis by eliminating cells with damaged DNA. This view is reinforced by the finding that many genes with pro-apoptotic function are absent or altered in cancer cells. The tumor suppressor p53 performs a significant role in apoptotic signaling by controlling expression of a host of genes that have pro-apoptotic or pro-survival function. The S_N1 DNA alkylating agent *N*-methyl-*N*′-nitro-*N*-nitrosoguanidine (MNNG) triggers apoptosis and the upregulation/phosphorylation of p53; however, the mechanism(s) governing MNNG-induced cell death remain unresolved. We observed that the human lymphoblastoid cell line WTK-1, which expresses mutant p53, shows far less sensitivity to the cytotoxic effects of MNNG than the closely related, p53-normal line TK-6. Exposure to 15 μM MNNG (LD50 at 24 h in TK-6) leads to a kinetically slower rate of apoptotic onset in WTK-1 cells compared to TK-6 as judged by viability assays and approaches that directly examine apoptotic onset. Similar results were obtained using an unrelated human lymphoblastoid line B310 expressing reduced levels of p53 due to E6 oncoprotein expression, indicating that MNNG activates both p53-dependent and -independent apoptotic mechanisms and that these two mechanisms are discernable by the rates which they trigger apoptotic onset. We document, during time points corresponding to peak apoptotic response in TK6, WTK-1, B310, and B310-E6, that these cell lines show marked decreases in mitochondrial transmembrane potential and increases in cytochrome *c* within the cytosolic fraction of MNNG-treated cells. Consistent with these events, we observed that both caspase-9 and -3 are activated in our panel of lymphoblastoid cells after MNNG exposure. We also found, using both broad spectrum and specific inhibitors, that blocking caspase activity in TK-6 and B310 cells had a significant effect on apoptotic advance, but that this treatment had no effect on entry of WTK-1 or B310-E6 cells into apoptosis. Finally, the PARP inhibitors benzamide and 6(5H)-phenanthridinone exerted notable inhibition of PARP activity and the nuclear translocation of the mitochondrial protein AIF (apoptosis-inducing factor) in MNNG-treated cells; however, these compounds exhibited no detectable inhibitory effects on MNNG-induced death in human lymphoblastoid cells. These observations suggest that PARP activity is not required during MNNG-triggered apoptosis in this cell type. Taken together, our observations support the conclusion that MNNG activates multiple apoptogenic pathways that contain both common and unique mechanisms.

Keywords: *N*-Methyl-*N*′-nitro-*N*-nitrosoguanidine; Apoptosis; p53

Introduction

DNA damage can occur when cells are exposed to numerous forces or toxins originating from either exogenous or endogenous sources. Such genotoxic events activate many signaling pathways which serve to activate DNA repair mechanisms, halt cell cycle progression, or trigger advancement into programmed cell death (apoptosis). These damage response pathways exist to limit the accumulation of heritable genetic errors. Not surprisingly, a wide range of tumor cells are defective in one or more of the elements that comprise

* Corresponding author. Department of Biochemistry and Molecular Biology, Box 100245, University of Florida College of Medicine, Gainesville, FL 32610. Fax: +1-352-392-1445.
E-mail address: kbrown@ufscc.ufl.edu. (K.D. Brown).
[1] Present address: Department of Biochemistry and Molecular Biology and UF Shands Cancer Center, University of Florida College of Medicine, Gainesville, FL, USA.
[2] Present address: Pennington Biomedical Research Center, Baton Rouge, LA, USA.

0041-008X/$ - see front matter © 2004 Elsevier Inc. All rights reserved.
doi:10.1016/j.taap.2004.06.009

these genome damage response mechanisms. Thus, these pathways are crucial to limiting the occurrence of somatic mutations, maintaining genomic homeostasis, and repressing tumorigenesis (Hartwell et al., 1994).

Apoptosis is an orderly mechanism whereby cells respond to internal or external stimuli by activating pathways that ultimately result in cell death. Apoptosis plays a normal physiological role in tissue remodeling during development and the removal of damaged cells following injury. In a pathophysiological context, aberrant regulation of apoptosis has been linked to the process of tumorigenesis by allowing cancer cells to evade cell death stimuli triggered as a result of malignant alterations in cell physiology (Hickman et al., 2002; Shen and White, 2001). Thus, understanding mechanisms that control regulation of apoptosis has great benefits to the study of cancer etiology and the cellular programs that govern the cytotoxicity of many cancer therapeutics.

Two general apoptogenic signaling mechanisms exist within cells: One pathway is mediated by the binding of ligands, such as the Fas ligand (FasL), to its receptor (Fas/CD95/APO-1) (Sun et al., 1999). Fas/FasL then complexes with adaptor proteins FADD and FLIP-L, and the proform of the initiator caspase, procaspase-8, to form a macromolecular complex termed the death-inducing signaling complex (DISC) (Strasser et al., 2000). The formation of DISC results in the activation of caspase-8 in an autoproteolytic manner. The second pathway is activated by non-receptor-associated stimuli (i.e., chemical carcinogens, steroid hormones, genotoxic agents) and results in compromised mitochondrial integrity leading to the accumulation of cytochrome *c* within the cytosol. Cytosolic cytochrome *c* then complexes with the apoptosis adaptor protein Apaf-1, dATP, and the initiator caspase, procaspase-9, to form a macromolecular complex termed the apoptosome and the consequential proteolytic activation of caspase-9 (Pan et al., 1998a, 1998b). Ultimately, both activated caspase-8 and -9 converge upon the activation of effector caspases such as caspase-3 which ultimately propel cells into death (Shi, 2002).

Key players in the control of mitochondrial integrity are members of the Bcl2 family. While the exact mechanism by which these proteins act as agonists or antagonists in driving mitochondrial permeability is controversial, various models have been proposed. The mitochondrial permeability transition pore (PTP) is a multiprotein complex that spans the inner and outer mitochondrial membranes (Kroemer et al., 1998). This pore allows ions and small molecules to freely pass with limited selectivity, but responds to stimuli that control the mitochondrial transmembrane potential ($\Delta\Psi_m$) such as pH, cellular Ca^{2+} concentration, redox status of mitochondrial matrix, and so on. Evidence suggests that the Bcl2 family members Bax, Bcl2, Bcl-XL, and Bid are more abundant at the PTP and thus may control the $\Delta\Psi_m$ by altering mitochondrial permeability (Bauer et al., 1999; Brenner et al., 2000; Marzo et al., 1998; Zamzami et al., 2000).

It is also clear that p53 plays a prominent role in apoptosis. The observation that mouse ES cells expressing recombinant p53 molecules containing a mutant transactivation domain were unable to trigger apoptosis supports a role for p53-dependent transcription in apoptosis (Chao et al., 2000). Of note, several members of the Bcl2 family (i.e., Bcl2, Bcl-X_L, Bax, Noxa, Puma) are under the transcriptional control of p53 (for review, see Shen and White, 2001). Thus, p53 likely exerts its effects on apoptogenic signaling, at least in part, through transcriptional modulation of molecules that promote mitochondrial permeability.

Human lymphoblastoid cells (EBV-transformed peripheral B lymphocytes) undergo apoptosis following exposure to numerous genotoxins (Greenwood et al., 1998; Li et al., 2002; Morris et al., 1998; Yu et al., 1997). While the mechanisms responsible for this event are poorly characterized, p53 apparently plays a role in this process since p53-deficient cells generally display a delay in apoptotic onset following ionizing radiation (IR) exposure (Yu and Little, 1998; Yu et al., 1997). This finding has led to the notion that, in human lymphoblasts, IR (as well as perhaps other genotoxins) triggers both p53-dependent and -independent apoptogenic mechanisms.

Only recently have nitrosoureas, a class of DNA alkylating agents, been shown to trigger apoptosis (Hickman and Samson, 1999; Meikrantz et al., 1998; Ochs and Kaina, 2000; Yu et al., 2002). Hickman and Samson (1999) found that MNNG-induced apoptosis is not strictly dependent upon p53 function. Ochs and Kaina (2000) showed that caspase-3 is activated in response to the monofunctional nitrosourea MNNG and that inhibiting this caspase reduced the apoptotic response. More recently, it has been observed that high-dose (500 μM) MNNG exposure triggers apoptosis in mouse fibroblasts and cultured neurons (Yu et al., 2002). Further, this group found that MNNG-induced apoptosis was not dependent upon caspase activation; rather, poly(ADP-ribose) polymerase (PARP)-dependent translocation of the mitochondrial flavoprotein AIF (apoptosis-inducing factor) from the mitochondria to the nucleus was required to trigger cell death in response to MNNG. Nevertheless, in general, the mechanisms that trigger nitrosourea-induced apoptosis, and particularly the role of p53 in this process, remain poorly defined.

In this report we examined the role that p53 plays in MNNG-induced apoptosis. We show that human lymphoblastoid cells expressing either a mutant form or an ablated complement of p53 display heightened resistance to the cytotoxic effects of MNNG. Several lines of evidence indicate that in response to MNNG exposure, loss of p53 function leads to a slower onset of apoptosis compared to p53-proficient lymphoblasts. These findings indicate that MNNG-induced apoptosis in human lymphoblastoid cells is triggered by p53-dependent and -independent pathways separable by the relative kinetics of apoptotic onset. Further, we have observed that both pathways converge at the point of increased mitochondrial permeability and lead to activation of caspase-9 and -3. The use of caspase inhibitors partially blocked apoptotic onset in p53-proficient lymphoblasts but had no discernable effect in p53-mutant/ablated

lymphoblasts, suggesting that p53-dependent mechanisms rely more heavily on caspase-3 activity than p53-independent mechanisms. Further, we observed that catalytic inhibition of PARP failed to significantly block cell death in MNNG-treated lymphoblasts, indicating that, in this cell type, both p53-dependent and -independent apoptogenic pathways apparently do not require PARP function.

Experimental procedures

Cell culture and drug treatment

The human lymphoblastoid cell lines TK-6 (expresses wild-type p53) and WTK-1 (expresses mutant p53) have been previously described (Liber and Thilly, 1982) as well as the normal lymphoblastoid line B310 (Brown et al., 1997). B310 cells were transduced with amphitrophic retrovirus encoding the HPV E6 oncoprotein (Halbert et al., 1991) using routine technique (Beardsley et al., 2003). All lines were grown in suspension cultures at 37 °C in a 5% CO_2 atmosphere. Cells were maintained in exponential growth (1×10^5 to 1×10^6 cells/ml) in RPMI-1640 medium supplemented with 10% heat-inactivated fetal bovine serum (GIBCO), 100 μg/ml streptomycin, and 100 units/ml penicillin. B310-E6 cells were maintained in complete growth media supplemented with 100 mg/ml G418.

MNNG (Aldrich) was dissolved in 0.1 M Na-acetate (pH 5.0) at a stock concentration of 10 mM and stored at −80 °C. MNNG was added to cell cultures at the indicated concentration for 1 h at 37 °C in a CO_2 incubator. After drug exposure, cells were rinsed extensively with PBS, refed on complete growth media, and returned to the incubator. Alternatively, cells were exposed to 10 Gy of γ-radiation from a 137 Cs source (Gammacell 1000, Atomic Energy of Canada Ltd; dose rate = 318 rad/min).

For caspase inhibition experiments, z-VAD-fmk and z-DEVD-fmk (R&D Systems, Inc.) were added to cell cultures at a final concentration of 100 μM 1 h before and during MNNG treatment, and was added again after MNNG treatment and remained in the culture media until cells were harvested. The PARP inhibitors PHT [6(5H)-phenanthridinone] and BA (benzamide) were purchased from Biomol and stocks of each were prepared in DMSO and stored at −20 °C before use. Treatment of cells with PARP inhibitors was done in a similar manner to that outlined for caspase inhibitors.

Cell viability

Cell viability was determined by MTS assay using CellTiter 96 as directed by the manufacturer (Promega). Cells were seeded into 96-well plates and the indicated concentration of MNNG was added for 1 h. Subsequently, cells were rinsed once in PBS and refed with 100 μl of complete growth medium. Cells were cultured for the indicated period of time and following this, 15 μl of MTS (3-(4,5-dimethylthiazol-2-yl)-5-(3-carboxymethoxyphenyl)-2-(4-sulphophenyl)-2H-tetrazolium) reagent was pipetted into each well and the plate incubated at 37 °C for 4 h. After incubation, absorbance was measured using a microplate spectrophotometer. Each independent experiment represents at least four separate measurements.

Immunoblot analysis

Immunoblotting was conducted as previously outlined (Adamson et al., 2002). Cells were harvested and lysates prepared by resuspending washed cell pellets in SDS lysis solution (125 μM Tris–HCl, pH 7.5/5 μM EDTA/5 μM EGTA/10 μM b-glycerolphosphate/10 μM NaF/10 μM Na-pyrophosphate/1.0% SDS) for 15 min on ice, and then placed in a boiling water bath for 5 min. Lysates were then briefly sonicated and cleared by centrifugation (1500 × *g*/2 min). Protein concentrations were determined using the BCA protein assay (Pierce) and lysates were stored at −80 °C. Before electrophoresis, appropriate volume of cell lysate was diluted in 3× SDS-sample buffer (150 μM Tris–HCl, pH 6.8, 10% β-mercaptoethanol, 20% glycerol, 3% SDS, 0.01% bromphenol blue, 0.01% pyronin-Y) and boiled for 2 min. Proteins were resolved on 10% SDS-polyacrylamide gels and electrotransferred onto nitrocellulose membranes. After transfer, the membranes were probed with antibodies directed against p53 (DO-1, PharMingen), $p21^{waf1/cip1}$ (Upstate Biotechnology), anti-procaspase- 9 and anti-cleaved caspase-3 (Cell Signaling Technology), and PARP (F2, Santa Cruz Biotechnology), tubulin (DM1A, a gift of Dr. D.W. Cleveland), actin (Chemicon), anti- poly(ADP-ribose) (Biomol), SMC1 (A300-055A, Bethyl Laboratories), or AIF (Ab-3, NeoMarkers). Peroxidase-conjugated secondary antibodies were obtained from Kirkegaard and Perry Laboratories. Immunoreactivity was visualized by chemiluminescence and recorded on X-ray film.

Terminal deoxynuclotidyl-mediated dUTP nick end labeing (TUNEL) analysis

Apoptosis was quantitatively measured using the In Situ Cell Death Detection Kit as outlined by manufacturer (Roche Molecular Biochemicals). Drug-treated cells were harvested at indicated time points, washed in PBS, fixed for 1 h at room temperature in 4% paraformaldehyde diluted in PBS, and subsequently permeabilized for 2 min at 4 °C in 0.1% Na-citrate/0.1% Triton-X 100. Cells were then washed twice in PBS containing 1% bovine serum albumin (BSA) and resuspended in 50 μl of deoxynucleotidyl transferase reaction buffer containing 1.2 μM fluorescein isothiocyanate transferase and incubated at 37 °C for 1 h. Finally, cells were washed once in PBS with 1% BSA, analyzed using a Becton-Dickinson FACScalibur flow cytometer and data analyzed using CellQuest software. As previously outlined (Walker et al., 1999), positive staining was assigned by setting gates at the highest staining 5% of cells within a population of mock-treated cells. Treated cells showing staining equal or greater than this value were scored as TUNEL positive.

Annexin V analysis

Either untreated or MNNG-treated cells were dually stained for annexin V and propidium iodide using the Annexin V-FITC Apoptosis Detection Kit I (BD Biosciences) according to the manufacturer's protocol. Briefly, following drug treatment, 1×10^5 cells were pelleted and washed once with ice-cold PBS and resuspended 100 μl of binding buffer (10 μM Hepes, pH 7.4, 150 μM NaCl, 5 μM KCl, 1 μM $MgCl_2$, and 2 μM $CaCl_2$). Subsequently, 5 μl of Annexin V-FITC and PI was added to the cells that were then incubated for 15 min at RT in the dark. After incubation, 400 μl of binding buffer was added to the stained cells and the cells analyzed by flow cytometry. Data analysis was conducted using Cell Quest software.

Fluorescence microscopy

Either untreated or MNNG-treated cells were applied to glass coverslips using a Cytospin 4 cytocentrifuge (Thermo Shandon). Subsequently, cells were fixed by immersion in cold (−20 °C) methanol, washed with PBS, and stained with Hoechst 33258 (0.1 mg/ml final concentration) diluted in PBS. Coverslips were then mounted onto glass slides and DNA morphology was assessed. Cells were photographed using a Leitz microscope equipped with epifluorescence optics and a SPOT CCD camera.

Mitochondrial membrane potential measurements

Mitochondrial membrane potential measurements were conducted using a modification of the method outlined by Antonicka et al. (1999). MNNG-treated and untreated cells (3×10^7) were harvested, washed three times in cold PBS, and resuspended in 1 ml of cold KCl medium (80 μM KCl/10 μM Tris−HCl, pH 7.4/3 μM $MgCl_2$/1 μM EDTA/5 μM KH_2PO_4) and 10 ml of 4 μM digitonin was subsequently added. After this, cells were placed on ice for 5 min and subsequently harvested by centrifugation and resuspended in 1 ml cold KCl medium. Tetramethylrhodamine Methyl Ester (TMRM) (20 nM final concentration) was added, cells incubated at room temperature for 10 min, and fluorescence quantified by flow cytometry. As controls, cells were subjected to flow cytometry without added TMRM (to establish baseline fluorescence) and the uncoupling agent carbonyl cyanide *p*-trifluoromethoxyphenylhydrazone (FCCP) (50 nM final concentration) was added 1 min before measuring TMRM fluorescence to induce complete loss of mitochondrial transmembrane potential.

Cell fractionation

Fractionation of human lymphoblastoid cells was accomplished using the method outlined by Karpinich et al. (2002). At the indicated time points after MNNG treatment, cells were harvested by centrifugation, washed once in PBS, and then resuspended in 1 ml of ice-cold Buffer A (20 μM Hepes-KOH, pH 7.5/10 μM KCl/1.5 μM $MgCl_2$/1 μM EDTA/0.1 μM phenylmethylsulfonyl fluoride/10 μg/ml each aprotinin and pepstatin). After resuspension, cells were kept on ice for 15 min and then lysed by 70 passages through a 26-gauge needle. The lysates were then centrifuged at $1000 \times g$ for 5 min at 4 °C and the resultant pellet and supernatant fractions separated. The supernatant was then centrifuged at $10\,000 \times g$ for 15 min at 4 °C. The cleared cytosolic fraction was concentrated using Centricon YM-10 devices (Millipore).

For immunoblot analysis of isolated nuclei, cells were separated into nuclear and cytoplasmic fractions using NE-PER Nuclear and Cytoplasmic Extraction Reagents as outlined by the manufacturer (Pierce). After lysing cells with supplied buffers, nuclei were harvested by centrifugation in a microcentrifuge (5 min; $16\,000 \times g$; 4 °C) and stored at −80 °C before immunoblot analysis.

Caspase activity analysis

Caspase-9 and -3 activity was measured using the Caspase Colorimetric Assay Kit as outlined by the manufacturer (R&D Systems). At indicated time points, cells were collected by centrifugation and subsequently lysed by the addition of the supplied ice-cold lysis buffer. The lysate was incubated on ice for 15 min, then cleared by centrifugation ($10\,000 \times g$, 1 min) and protein concentrations subsequently determined using the BCA protein assay. Cell extracts (40 μg total protein) were incubated with 2× reaction buffer and 40 μM DEVD-pNA (to measure caspase-3 activity) or LEHD-pNA (to measure caspase-9 activity) peptide substrate in a total volume of 100 μl at 37 °C for 1 h. Levels of released (cleaved) chromophore were measured by spectrophotometry.

Results

Characterization of human lymphoblast lines expressing wild-type, mutant, or ablated p53

The primary focus of this study was to elucidate the role that p53 plays in triggering apoptosis in response to the monofunctional alkylating agent *N*-methyl-*N*′-nitro-*N*-nitrosoguanidine (MNNG). Our first objective was to assemble a panel of isogenically matched human lymphoblastoid cells with defined p53 status. We obtained the lymphoblastoid line TK-6 (expresses wild-type p53) and its derivative, WTK-1 (homozygous for a mutation in codon 237 of the p53 gene product) (Xia et al., 1995) from Dr. John Little (Harvard School of Public Health). Further, we have derived a cell line from the normal human lymphoblastoid line B310 (Brown et al., 1997) by transducing this line with amphitrophic retrovirus that express the E6 protein of human papilloma virus (HPV). This cell line is designated B310-E6.

Because ionizing radiation (IR) exposure results in the upregulation of cellular p53 abundance which is generally maintained at low levels, we exposed TK-6, WTK-1, B310, and B310-E6 cells to 10 Gy of IR and formed extracts 4 h after irradiation. Comparing p53 levels in unirradiated and irradiated TK-6 and B310 cells, we observed a 3- to 4-fold increase in p53 abundance following γ-irradiation (Fig. 1, top). In WTK-1, we observed a constitutively increased level of p53 that was unaltered by irradiation. This is consistent with previous findings (Xia et al., 1995), and is indicative of the mutant form of this protein expressed in WTK-1 cells. We failed to detect p53 in either unirradiated or irradiated B310-E6 cells. This substantially reduced level of p53 expression is consistent with E6 functioning as a ubiquitin ligase that targets p53 for proteolysis (Scheffner et al., 1993).

Next, we tested for p53 function by examining $p21^{waf1/cip1}$ levels in response to IR. This protein is an inhibitor of cyclin-dependent kinases and is upregulated in a p53-dependent manner in response to irradiation (el-Deiry et al., 1993). Consistent with normal p53 function, we observed robust upregulation of $p21^{waf1/cip1}$ in TK-6 and B310 following IR (Fig. 1, middle). Further, no clear increase in $p21^{waf1/cip1}$ was observed in irradiated WTK-1 and B310-E6 cells consistent with defective p53 function. In sum, these studies confirm that TK-6 and B310 express functional p53, WTK-1 expresses a nonfunctional p53 mutant, and B310-E6 cells express a reduced complement of p53.

p53-deficient lymphoblasts show reduced sensitivity to MNNG

Our first test to examine the role that p53 plays in triggering apoptosis in response to the monofunctional alkylating agent MNNG was to evaluate the sensitivity of human lymphoblastoid cells to this drug. TK-6 and WTK-1 cells were treated with concentrations of MNNG ranging from 20 nM to 20 μM for 1 h and cell viability was assessed 72 h after drug exposure using an MTS assay (Fig. 2A). This analysis indicated that TK-6 undergo a dramatic drop in viability when treated with doses of MNNG from

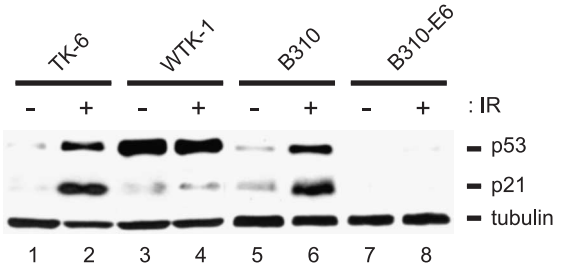

Fig. 1. Characterization of p53 status in human lymphoblastoid cell lines. TK-6 (lanes 1, 2), WTK-1 (lanes 3, 4), B-310 (lanes 5, 6), and B310-E6 cells were either untreated (lanes 1, 3, 5, 7) or exposed to 10 Gy of IR (lanes 2, 4, 6, 8). After irradiation (4 h), cells were harvested, washed extensively, and extracts formed. Subsequently, lysates were subjected to immunoblot analysis with anti-p53 (top), anti-$p21^{waf1/cip1}$ (middle), or anti-tubulin (bottom) to assure equivalent protein loading.

200 nM (approximately 100% viability) to 1 μM (35.5% viability, ±5.3 SD). Further reduction in TK-6 viability was observed at 20 μM MNNG (23.8% viability, ±4.6% SD). In contrast, we observed that WTK-1 treated with doses up to 5 μM MNNG maintained high viability (≥80%). WTK-1 cells treated with higher doses of MNNG (10 or 20 μM) showed reduced viability (68.6 ± 3.0% SD and 42.3 ± 3.8% SD, respectively).

To assure that the differences in response to MNNG in TK-6 and WTK-1 cells are attributable to p53 status, we conducted parallel experiments on B310 and B310-E6 cells. Over the dose range tested, we observed that B310-E6 cells exhibit diminished sensitivity to MNNG when compared to B310 cells (Fig. 2B) and is similar to the response observed in WTK-1. In sum, these observations indicate that lost or diminished p53 function renders human lymphoblastoid cells less sensitive to the cytotoxic effects of MNNG.

To verify that observed decreases in cell viability in response to MNNG treatment were due to apoptosis, we collected TK-6 and WTK-1 cells treated with various doses of MNNG 72 h after drug treatment. Cell lysates were formed and immunoblotted with anti-poly(ADP-ribose) polymerase (PARP) (Fig. 2C). Cleavage of the full-length approximately 116-kDa PARP polypeptide into approximately 85-kDa N-terminal and approximately 25-kDa C-terminal fragments is a well-characterized molecular marker of programmed cell death (Casciola-Rosen et al., 1996). We observed cleavage of PARP in TK-6 cells treated with 20 and 100 nM MNNG. Strikingly, TK-6 treated with higher drug concentrations showed complete cleavage of PARP, consistent with a robust apoptotic response. WTK-1 cells showed no observable PARP cleavage at 20 and 100 nM MNNG (Fig. 2D). Weak accumulation of the cleaved form of PARP was evident in cells treated with 200 nM MNNG and, at higher drug doses, increased PARP cleavage was observed in WTK-1. However, unlike MNNG-treated TK-6, complete cleavage of full-length PARP was never observed in WTK-1 treated with the outlined doses of MNNG at the 72-h time point. Analysis of B310 cells treated with 100 nM MNNG showed complete PARP cleavage (Fig. 2E). B310-E6 cells treated with 100 nM MNNG showed quantitatively less PARP cleavage than similarly treated B310 cells, and PARP cleavage in this p53-ablated line was enhanced in cells exposed to 15 μM MNNG. Taken together, these findings indicate that p53-mutant/ablated WTK-1 and B310-E6 cells show a higher threshold for the cytotoxic effects of MNNG than normal (TK6 and B310) lymphoblasts, and that this cytotoxicity is attributable to the MNNG-induced triggering of apoptosis in this cell type.

MNNG triggers apoptosis through p53-dependent and -independent mechanisms

Whereas WTK-1 cells exhibit reduced sensitivity to MNNG, we reasoned that employing these cells to study the role of p53 in MNNG-induced apoptosis would necessi-

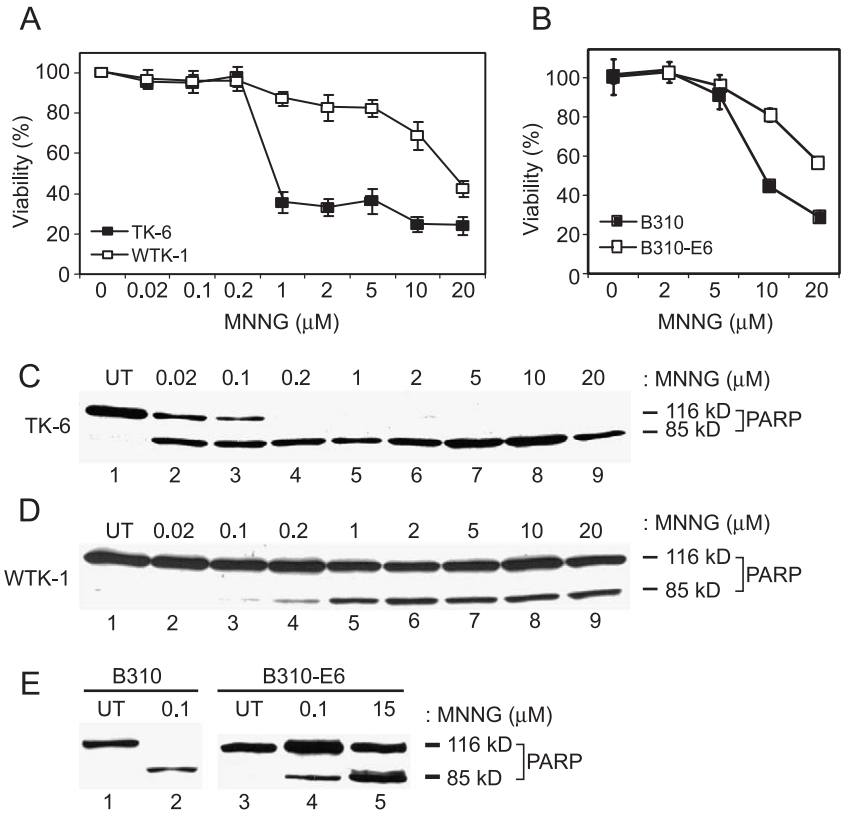

Fig. 2. p53-deficiency results in reduced sensitivity to MNNG. (A) TK-6 (■) and WTK-1 (□) cells were treated with the indicated dose of MNNG for 1 h at 37 °C. Following 72-h incubation, cell viability was assessed using an MTS assay. Graphed is the mean of six independent experiments, error bars = 1 SD. (B) B310 (■) and B310-E6 (□) cells were treated with the indicated dose of MNNG and 72 h later cell viability was determined by MTS assay. Graphed is the mean of three independent experiments. (C) TK-6 cells were either untreated (lane 1) or were treated with the indicated dose of MNNG for 1 h (lanes 2–9). Following 72-h incubation, cells were harvested, extracts formed and immunoblotted with anti-PARP. The full-length approximately 116-kDa PARP protein and the apoptosis-associated approximately 85-kDa fragment are indicated. (D) WTK-1 cells were either untreated (lane 1) or were treated with the indicated dose of MNNG for 1 h (lanes 2–9). Following 72-h incubation, cells were harvested, extracts formed and immunoblotted for PARP. (E) B310 (lanes 1, 2) and B310-E6 cells (lanes 3–5) were either untreated or treated with the indicated dose of MNNG for 1 h. Cells were harvested after 72 h incubation, extracts formed and immunoblotted with anti-PARP.

tate use of relatively high doses of MNNG. Thus, we decided to establish the dose of MNNG corresponding to the LD50 in TK-6 cells. This was determined by exposing TK-6 to a range of MNNG doses (2.5–100 μM) and quantifying viability 24 h after drug addition (Fig. 3A). From this analysis we determined that, in TK-6 cells, the LD50 for MNNG at 24 h is 15 μM.

Next, we treated both TK-6 and WTK-1 cells with 15 μM and assessed cell viability at 1-day intervals for 6 days after drug treatment. These results indicate that TK-6 undergo a rapid loss in viability (21.8% viability, ±3.9% SD) 2 days after 15 μM MNNG exposure (Fig. 3B). No further dramatic decrease in cell viability was observed in TK-6 cells 3–6 days after MNNG treatment. In contrast, WTK-1 showed no detectable loss in viability 1 day after 15 μM MNNG treatment. Two days after drug, these p53-mutant cells showed reduced viability (65.2% viability, ±4.7% SD) and this slow diminishment in viability continued until day 6 when WTK-1 cells exhibited levels of viability consistent with treated TK-6 cells (15.7 ± 1.9% and 13.3 ± 1.7%, respectively). These findings indicate that loss of viability in TK-6 cells treated with high doses of MNNG is a rapid process while the related p53-mutant line WTK-1 shows a more gradual decline in cell viability.

Again, to assure that these phenotypic differences in rates of MNNG-induced cell death were attributable to p53, we conducted parallel experiments on B310 and B310-E6 cells. The results of this experiment indicate that B310-E6 cells display a slower onset of cell death following exposure to 15 μM MNNG when compared to B310 cells (Fig. 3C). Taken together, these findings indicate that, in response to 15 μM MNNG, p53-deficient lymphoblasts trigger cell death in a kinetically slower fashion than wild-type lymphoblasts.

To directly examine apoptotic onset in TK-6 and WTK-1 cells following MNNG exposure, we harvested cells at various times after 15 μM MNNG exposure, formed cell lysates, and immunoblotted these with anti-PARP. In TK-6 lysates, we detected significant cleavage of this protein 12 h after MNNG exposure and, by the 36-h post-MNNG time point, complete cleavage of PARP was observed (Fig. 3D). In WTK-1 lysates, slight PARP cleavage was observed in cells harvested 36 h after MNNG, and notably greater

digestion of this polypeptide occurred at later time points (Fig. 3E).

To independently assess apoptotic onset, we analyzed TK-6 and WTK-1 cells at various times after MNNG by TUNEL analysis (Fig. 3F). The percentage of the drug-treated cells in apoptosis was quantified by flow cytometry (van Engeland et al., 1998). We found 1 day after 15 μM MNNG exposure that 72.7% (±6.8% SD) of TK-6 cells were TUNEL-positive, and this percentage rose to 92.7% (±4.0% SD) 48 h after drug. Again, WTK-1 cells displayed a kinetically slower advance into apoptosis following exposure to 15 μM MNNG. For example, 1 day after drug, 34.7% (±4.5% SD) of WTK-1 cells exhibited positive TUNEL staining and this TUNEL-positive percentage rose

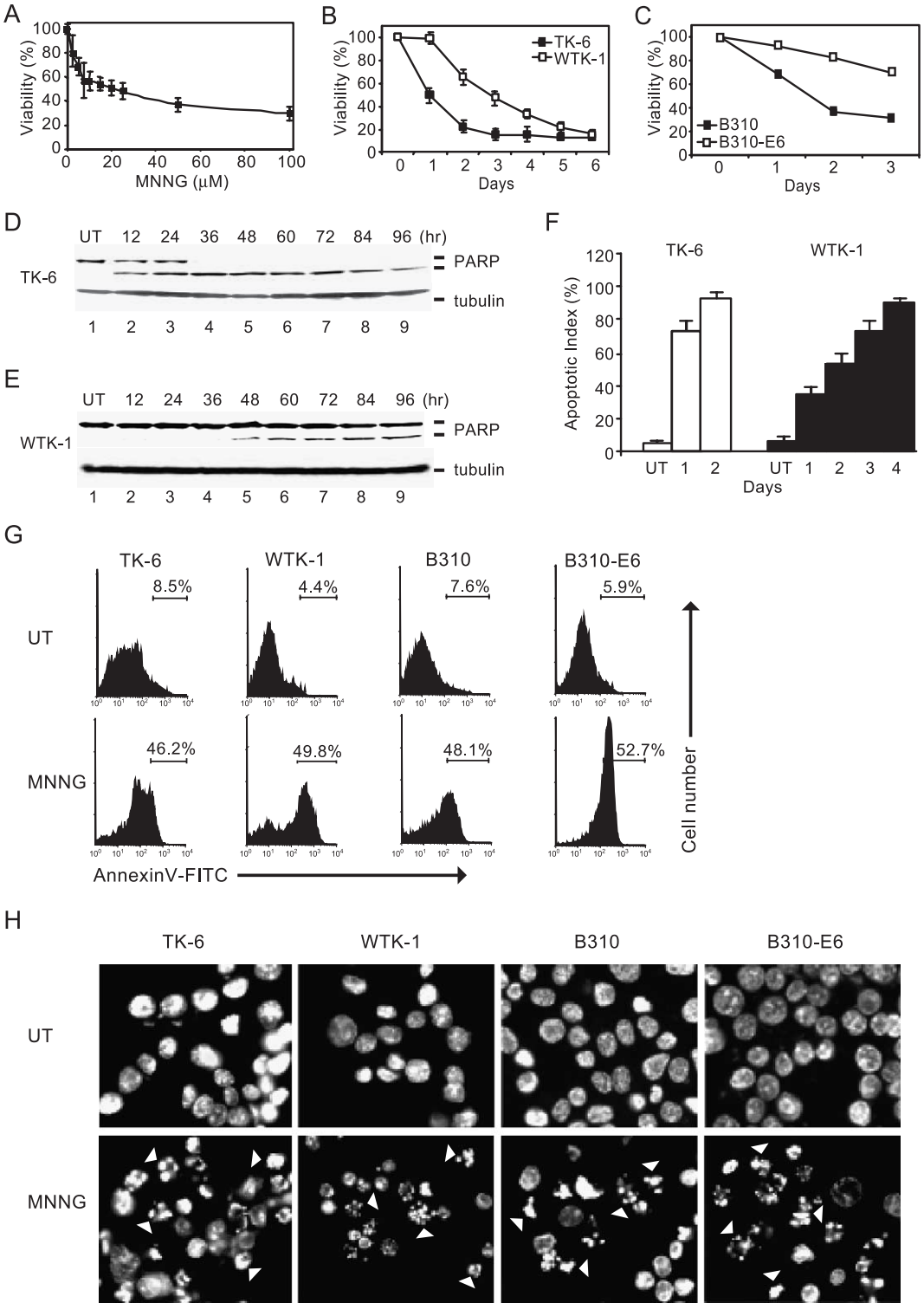

gradually until day 4 where 90.4% (±3.1% SD) of these cells had triggered apoptosis.

Next, we assessed apoptotic onset by conducting annexin V analysis which scores phosphatidylserine redistribution to the outer plasma membrane. This event is a well-established early marker of apoptosis that can be quantified in a population of cells using flow cytometry. Annexin V staining was examined in TK-6 and B310 cells 24 h after 15 μM MNNG exposure. Alternatively, WTK-1 and B310-E6 cells were analyzed 72 h after drug. We observed, in each cell line a dramatic increase in annexin V staining in response to MNNG treatment (Fig. 3G). In general, approximately 50% of each population displayed positive annexin V staining at the indicated time point after 15 μM MNNG exposure.

Finally, we examined nuclear morphology in MNNG-treated lymphoblasts. In untreated lymphoblasts, each line displayed normal nuclear morphology when stained with Hoechst 33258 and observed by fluorescence microscopy. In contrast, in populations of MNNG-treated cells we observed numerous cells showing irregularly shaped nuclei containing condensed chromatin (Fig. 3H) that are indicative of apoptosis. In sum, these findings firmly indicate that MNNG is a potently apoptogenic genotoxic agent. Further, like response to IR (Yu and Little, 1998), MNNG activates a rapid p53-dependent apoptogenic pathway(s) and a kinetically slower p53-independent pathway(s).

Both p53-dependent and -independent pathways increase mitochondrial permeability and activate caspase-3 and -9

Various stimuli trigger apoptosis through mitochondrial-dependent and mitochondrial-independent mechanisms. To further characterize the mechanisms responsible for MNNG-induced apoptosis, we measured mitochondrial transmembrane potential ($\Delta\Psi_m$) after MNNG treatment in TK-6 and WTK-1 cells using the stain tetramethylrhodamine (TMRM). Accumulation of TMRM within mitochondria is proportional to $\Delta\Psi_m$ and, thus, is a commonly employed method for measuring mitochondrial integrity by FACS (see Rasola and Geuna, 2001). We observed that TK-6 treated with 15 μM MNNG displayed a rapid drop in $\Delta\Psi_m$ 24 h after MNNG (17.9 ± 4.6% SD of untreated controls) (Fig. 4A). Transmembrane potential measured in TK-6 2–4 days following 15 μM MNNG remained very low (<10% of untreated cells). Conversely, and consistent with the kinetically slower rate of apoptotic onset observed in WTK-1, we observed that these p53-mutant lymphoblasts showed a slow decrease in $\Delta\Psi_m$ which reached its lowest point (25.6% of untreated controls) 4 days after 15 μM MNNG treatment.

To confirm that drops in mitochondrial transmembrane potential were leading to increased mitochondrial permeability, we assayed for the presence of cytochrome *c* in the cytosol of MNNG-treated human lymphoblasts. Hypotonically lysed cells were fractionated by centrifugation and the

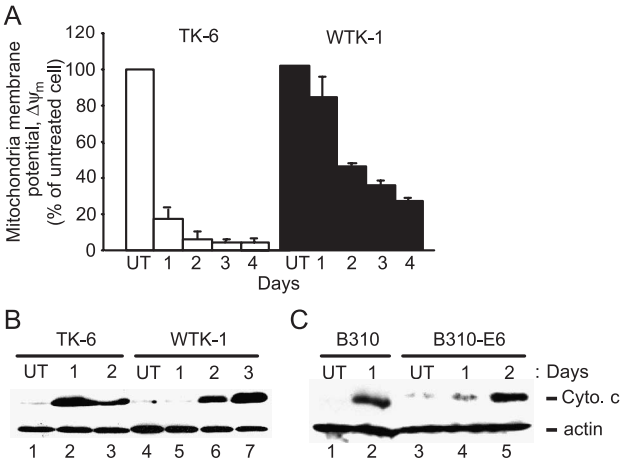

Fig. 4. Decreased mitochondrial transmembrane potential and increased mitochondrial permeability occur during both p53-dependent and -independent apoptosis. (A) TK-6 (open bars) and WTK-1 (filled bars) were treated with 15 μM MNNG and, at the indicated time point, relative mitochondrial membrane potential was determined by TMRM staining. Graphed is the mean of three independent experiments, error bars = 1 SD. (B) TK-6 cells (lanes 1–3) and WTK-1 cells (lanes 4–7) were either untreated (lanes 1, 4) or treated with 15 μM MNNG (lanes 2, 3, 5, 6, 7) and at the indicated time point after drug exposure were hypotonically lysed and the cytosolic fraction isolated by centrifugation. Subsequently, equivalent loadings of these cytosolic fractions were subjected to immunoblot analysis with anti-cytochrome *c* (top) or anti-actin (bottom) to assure equivalent loading. (C) B310 (lanes 1, 2) and B310-E6 (lanes 3–5) were treated, fractionated, and analyzed in (B).

Fig. 3. p53-deficiency results in a kinetically slower rate of apoptotic onset following MNNG exposure. (A) TK-6 cells were treated with the indicated dose of MNNG and 24 h later cell viability was quantified by MTS assay. This experiment indicated that the LD_{50} for MNNG is 15 μM at 24 h in this cell line. Graphed is the mean of four independent experiments, error bars = 1 SD. (B) TK-6 (■) and WTK-1 (□) cells were treated with 15 μM MNNG for 1 h and cell viability was measured by MTS assay at the indicated time point after drug exposure. Graphed is the mean of four independent experiments, error bars = 1 SD. (C) B310 (■) and B310-E6 (□) cells were treated with 15 μM MNNG and cell viability was determined by MTS assay at the indicated time point. Graphed is the mean of three independent experiments, error bars = 1 SD. (D) TK-6 cells were either untreated (lane 1) or were treated with 15 μM MNNG, harvested at the indicated time point, and extracts formed (lanes 2–9). Extracts were subsequently immunoblotted with anti-PARP (top) or tubulin (bottom) to confirm equivalent loading. (E) WTK-1 cells were either untreated (lane 1) or treated with 15 μM MNNG (lanes 2–9), harvested at the indicated time point, extracts formed and immunoblotted with anti-PARP (top) or tubulin (bottom). (F) TK-6 (open bars) and WTK-1 (filled bars) cells were treated with 15 μM MNNG and at the indicated time point were processed for TUNEL assay. The percentage of apoptotic cells in each population (apoptotic index) was determined by flow cytometry. Graphed is the mean of three independent experiments, error bars = 1 SD. (G) Indicated lymphoblast lines were either untreated or treated with 15 μM MNNG and harvested either 24 h (TK-6, B310) or 72 h (WTK-1, B310-E6) after drug. Subsequently, cells were dually stained with annexin V and PI, and subsequently analyzed by flow cytometry. The percentage of cells displaying positive annexin V staining in each population is indicated. (H) Indicated lymphoblast lines were either untreated or treated with 15 μM MNNG and harvested either 24 h (TK-6, B310) or 72 h (WTK-1, B310-E6) after drug. Cells were then applied to glass coverslips, fixed, and stained with Hoechst 33,258 to reveal nuclei. Cells were viewed on an epifluorescence microscope and photographed. Note presence of irregularly shaped apoptotic nuclei (arrowheads).

cytosolic fraction subjected to immunoblot analysis with anti-cytochrome *c*. We observed accumulation of cytochrome *c* within the cytosol of treated TK-6 and WTK-1 cells (Fig. 4B). However, we noted a slower accumulation of cytochrome *c* in the cytosol of WTK-1 cells when compared to cytosolic extracts prepared from MNNG-treated TK-6 cells. These findings are consistent with the kinetically slower triggering of apoptosis in WTK-1 cells and correlates with our analysis of mitochondrial transmembrane potential. We also analyzed cytosolic cytochrome *c* levels in B310 and B310-E6 cells (Fig. 4C). Like TK-6, we observed accumulation of cytochrome *c* in the cytosol of MNNG-treated B310 cells 24 h after drug exposure. Similar to WTK-1, p53-ablated B310-E6 cells showed a kinetically slower accumulation of cytochrome *c* within the cytosolic fraction. These findings lead us to conclude that increased mitochondrial permeability occurs as a result of triggering either p53-dependent or p53-independent apoptotic pathways in MNNG-treated human lymphoblasts.

Increased mitochondrial permeability drives apoptosis through promoting apoptosome formation and consequential activation of caspase-9 (Pan et al., 1998a, 1998b). We examined cleavage of the procaspase-9 protein in extracts from TK-6 and WTK-1 cells during time points corresponding to peak apoptotic activity (24 h for TK-6, 72 h for WTK-1). Immunoblotting revealed that the 47-kDa proform of this protease was cleaved into the 37- and 35-kDa active forms in both cell lines in response to MNNG treatment (Fig. 5A). Direct analysis of caspase-9 activity in extracts of MNNG-treated TK-6 and WTK-1 cells showed a greater than 2-fold activation in this protease during peak MNNG-induced apoptotic response (Fig. 5B). Similar results were observed in B310 and B310-E6 cells (data not shown).

Caspase-9 cleaves and hence activates caspase-3, a well-characterized effector caspase. Immunoblot analysis of extracts from MNNG-treated TK-6 and WTK-1 cells with an antibody that specifically recognizes the active (cleaved)

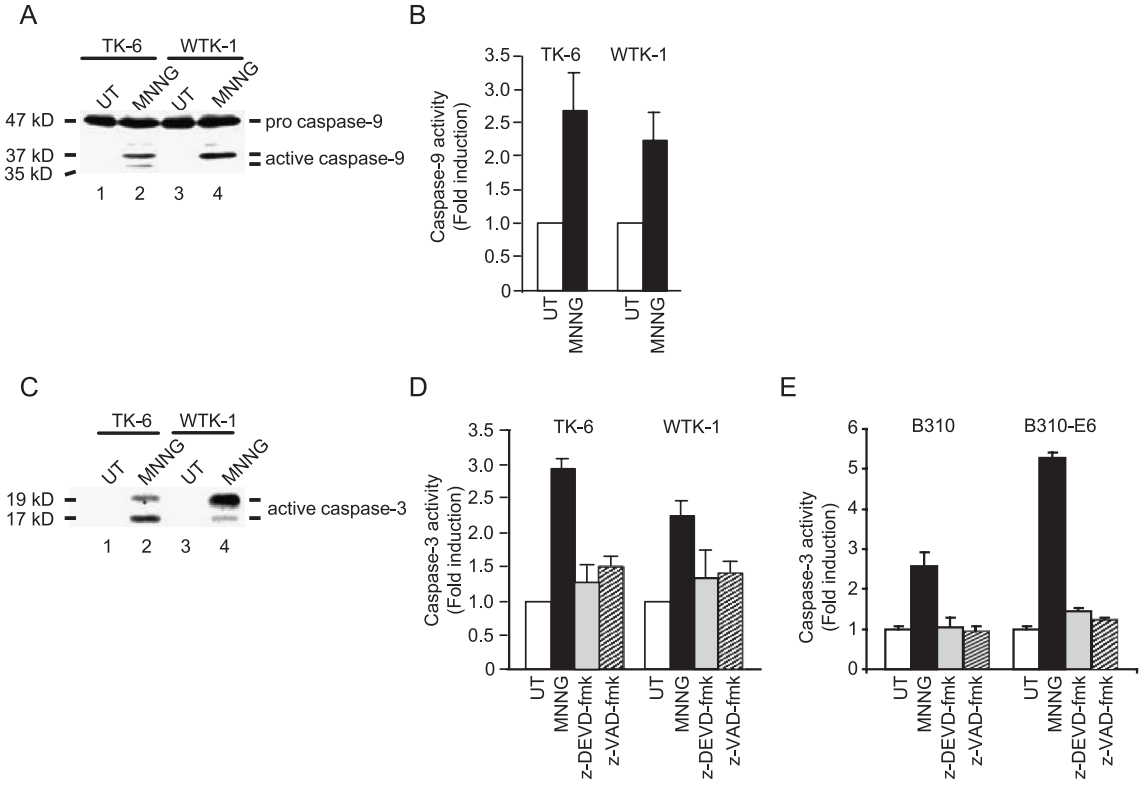

Fig. 5. Caspase-9 and -3 are activated by p53-dependent and -independent pathways in response to MNNG. (A) TK-6 (lanes 1, 2) and WTK-1 (lanes 3, 4) were either untreated (lanes 1, 3) or treated with 15 μM MNNG (lanes 2, 4). TK-6 were harvested 24 h after MNNG, WTK-1 were harvested 72 h after drug. Subsequently, lysates were formed and subjected to immunoblot analysis with anti-caspase-9. Indicated is the 47-kDa procaspase molecule and the cleaved 37- and 35-kDa forms of active caspase-9. (B) TK-6 and WTK-1 cells were either untreated (open bars) or treated with 15 μM MNNG (closed bars) and extracts formed at 24 h (TK-6) or 72 h (WTK-1) after MNNG treatment. Subsequently, relative caspase-9 activity was measured colorimetrically using a specific peptide substrate. Graphed is the mean of five independent experiments, error bars = 1 SD. (C) TK-6 (lanes 1, 2) and WTK-1 (lanes 3, 4) were either untreated (lanes 1, 3) or treated with 15 μM MNNG (lanes 2, 4). Lysates were formed and immunoblotted with an antibody that specifically detects the cleaved form of caspase-3. Indicated are the 19- and 17-kDa forms of active caspase-3. (D) TK-6 and WTK-1 cells were either untreated (open bars) or treated with 15 μM MNNG (closed bars) and extracts formed at 24 h (TK-6) or 72 h (WTK-1) after MNNG treatment. Where indicated, cells were pretreated with the 100 μM pan-specific caspase inhibitor z-VAD-fmk (shaded bars) or 100 μM caspase-3 inhibitor z-DEVD-fmk (crosshatched bars) before, during, and after MNNG treatment. Subsequently, relative caspase-3 activity was measured colorimetrically using a specific peptide substrate. Graphed is the mean of three independent experiments, error bars = 1 SD. (E) B310 and B310- E6 cells were treated and analyzed as in (D). Graphed is the mean of three independent experiments, error bars = 1 SD.

form of caspase-3 shows that this protease is cleaved into the active 19- and 17-kDa forms during response to MNNG (Fig. 5C). Similarly, direct analysis of this enzyme showed an approximate 3-fold increase in caspase-3 activity in TK-6 and an approximate 2.3-fold increase in MNNG-treated WTK-1 (Fig. 5D). We also analyzed MNNG-induced caspase-3 activity in both TK-6 and WTK-1 cells pretreated with the pan-specific caspase inhibitor z-VAD-fmk and the specific caspase-3 inhibitor z-DEVD-fmk to judge the efficacy of these compounds in human lymphoblastoid cells. We observed a significant decrease in caspase-3 activity in each line treated with either inhibitor (Fig. 5D). Again, these experiments were also performed on B310 and B310-E6 cells (Fig. 5E). These analyses also showed that MNNG induces a notable increase in caspase-3 activity in both lines and that this activity is significantly inhibited by either z-DEVD-fmk or z-VAD-fmk. In sum, these findings indicate that, regardless of p53 status, MNNG exposure results in increased mitochondrial permeability and downstream activation of both caspase-9 and -3.

Effects of caspase and PARP inhibitors on p53-dependent and p53-independent cell death

Others have reported that, in rodent cells, MNNG exposure triggers caspase-3-dependent apoptosis (Ochs and Kaina, 2000). To determine if such caspase dependency applies to both p53-dependent and -independent apoptogenic mechanisms in human lymphoblasts, we used z-VAD-fmk and z-DEVD-fmk to inhibit caspase activity in MNNG-treated cells. We observed that z-VAD-fmk reduced the percentage of apoptotic cells, as scored by TUNEL analysis, in populations of TK-6 treated with 15 μM MNNG (Fig. 6A). While this inhibitory effect is modest, z-VAD-fmk treatment resulted in a statistically significant inhibition of apoptotic onset in TK-6 ($P = 0.02$). (P values were calculated using a two-tailed Student's t test.) In contrast, we observed no statistically significant reduction in apoptotic onset in WTK-1, B310, or B310-E6 cells pretreated with z-VAD-fmk ($P > 0.05$). Using z-DEVD-fmk, we also observed a significant inhibition of MNNG-induced apoptosis in TK-6 ($P = 0.01$). Similarly, we observed that z-DEVD-fmk reduced apoptotic onset in B310-E6 cells ($P = 0.05$). Consistent with observations using z-VAD-fmk, we found that z-DEVD-fmk did not significantly inhibit apoptotic onset in either WTK-1 or B310-E6 cells.

The enzymatic activity of PARP is required for MNNG-induced apoptosis in mouse cell lines (Yu et al., 2002). To test if this enzyme is required for triggering apoptosis in MNNG-treated human lymphoblasts, we analyzed the requirement for PARP in MNNG-treated lymphoblastoid cells by using the well-characterized PARP inhibitors benzamide (BA) and 6(5H)-phenanthridinone (PHT) (Virag and Szabo, 2002). We confirmed that treatment of lymphoblasts with either 5 μM PHT or 50 μM BA for 1 h before, during, and after addition of MNNG abrogated the enzymatic activity of

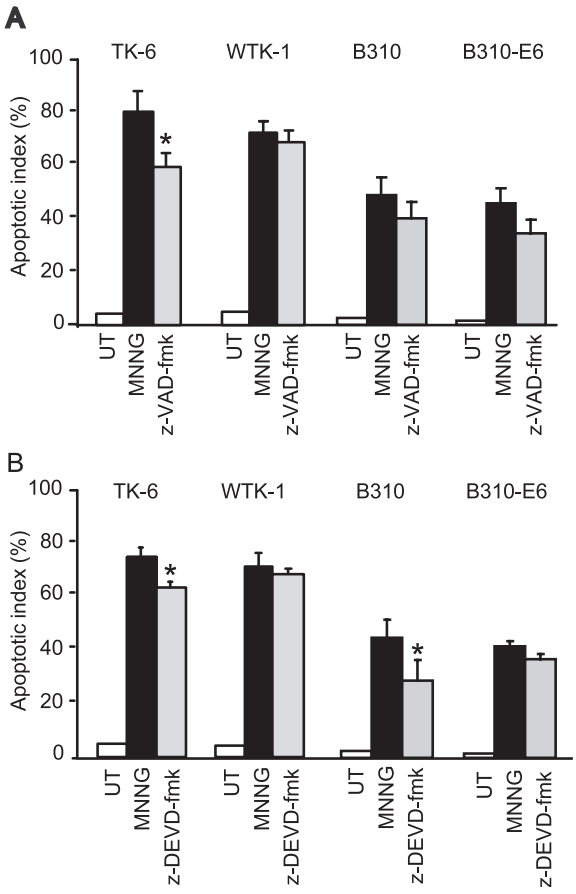

Fig. 6. p53-dependent apoptosis displays heightened dependency upon caspase activity versus p53-independent apoptosis. (A) TK-6 and WTK-1 cells were either untreated (open bars), treated with 15 μM MNNG (filled bars), or treated with a 100-μM concentration of the pan-specific caspase inhibitor z-VAD-fmk (shaded bars) before, during, and after MNNG treatment. TK-6 cells were harvested 24 h after MNNG and WTK-1 cells were harvested 72 h after drug. Subsequently, cells were processed for TUNEL analysis and the apoptotic index (percent of TUNEL-positive cells) was determined by flow cytometry. (B) Cells were treated and analyzed as outlined in A except that cells were treated with a 100-μM concentration of the caspase-3 inhibitor z-DEVD-fmk (shaded bars) before, during, and after MNNG treatment. In all cases, graphed is the mean of at least three independent experiments, error bars = 1 SD. Asterisks indicate $P \leq 0.05$.

PARP. This inhibitory effect was judged by the loss of immunoreactivity of an anti-poly(ADP-ribose) antibody to high-molecular-weight proteins that display ADP-ribosylation in untreated and MNNG-treated TK-6 and WTK-1 (Fig. 7A), as well as B310 and B310-E6 lymphoblasts (Fig. 7B). Yu et al. (2002) showed that inhibition of PARP activity blocked the nuclear translocation of AIF, a mitochondrial flavoprotein, from the cytosol to the nucleus. To test if inhibition of PARP activity also blocked this translocation in MNNG-treated lymphoblasts, we isolated nuclei from untreated and MNNG-treated TK-6 and WTK-1 cells that were incubated in either the presence or absence of 5 μM PHT. These isolated nuclei were then subjected to immunoblot analysis with either anti-AIF (Fig. 7C, top) or an antibody to the nuclear protein SMC1 (Fig. 7C, bottom).

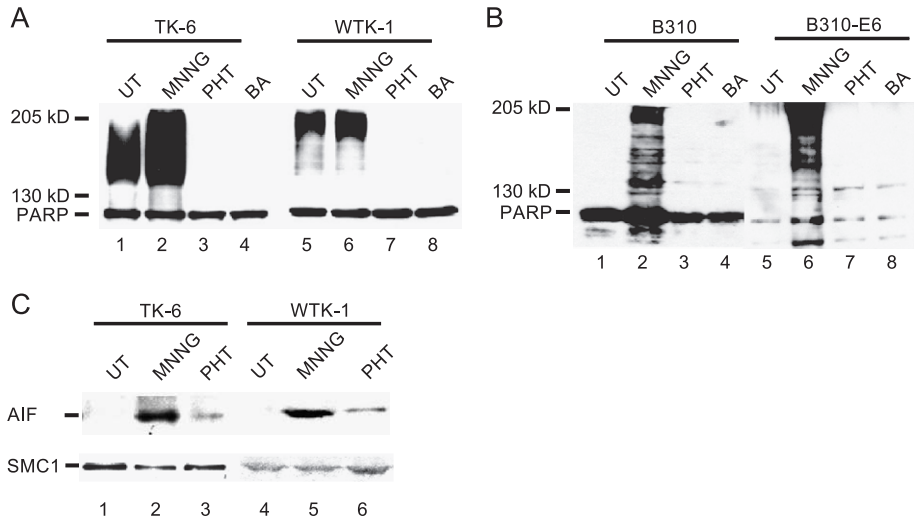

Fig. 7. Benzamide and 6(5H)-phenanthridinone effectively inhibit PARP activity in MNNG-treated human lymphoblasts. (A) TK-6 (lanes 1–4) and WTK-1 (lanes 5–8) cells were either untreated (lanes 1, 5), treated with 15 μM MNNG only (lanes 2, 6), pretreated with 5 μM 6(5H)-phenanthridinone (PHT) for 1 h before, during 15 μM MNNG treatment (lanes 3, 7), or pretreated with 50 μM benzamide (BA) for 1 h before, during, and after 15 μM MNNG treatment (lanes 4, 8). Following MNNG exposure, cells were washed, PARP inhibitors re-added to the medium, and cells harvested after incubation (24 h for TK-6, 72 h for WTK-1). Lysates were formed and immunoblotted with anti-poly(ADP-ribose). The ADP-ribosylated PARP molecule is indicated. (B) B310 (lanes 1–4) and B310-E6 cells (lanes 5–8) were treated and analyzed as outlined in A. (C) TK-6 (lanes 1–3) and WTK-1 (lanes 4–6) were either untreated (lanes 1, 4), treated with 15 μM MNNG only (lanes 2, 5), or treated with both 5 μM PHT and 15 μM MNNG (lanes 3, 6). After drug treatment (24 h for TK-6, 72 h for WTK-1), nuclei were isolated from each line, extracts formed and subjected to immunoblot analysis with anti-AIF (top) or the nuclear protein SMC1 (bottom) to confirm equal loading.

This set of experiments clearly indicated that 50 μM BA strongly inhibited but did not completely abrogate AIF accumulation within the nucleus of MNNG-treated lymphoblasts. Similar findings were observed in cells treated with 50 μM BA (data not shown).

Next, we tested if PHT or BA inhibited MNNG-induced cell death in our panel of human lymphoblasts. We found that a range of concentrations of either PHT (Fig. 8A) or BA (Fig. 8B) did not significantly diminish MNNG-induced loss in cell viability, as judged by MTS assays, in TK-6 cells treated with 15 μM MNNG. Similar results were observed in WTK-1 (Fig. 8C), B310 (Fig. 8D), and B310-E6 (Fig. 8E). To confirm that these decreases in viability observed in cells treated with MNNG with or without PARP inhibitors correspond to apoptotic onset, we conducted annexin V analysis (Fig. 8F). Consistent with previous experiments (see Fig. 3G), we observed that approximately 50% of MNNG-treated TK-6 and B310 cells stain annexin V-positive 24 h after 15 μM MNNG treatment. Co-culture of these cells with either 5 μM PHT or 50 μM BA failed to result in any marked decrease in annexin V staining in these cells. Similar results were obtained when B-310 cells were tested at 24 h after MNNG, and WTK-1 and B310-E6 cells were tested 72 h after this drug. Taken together, these findings indicate that PHT and BA, when used at concentrations that measurably reduce PARP activity and nuclear accumulation of AIF in MNNG-treated human lymphoblasts, seemingly do not inhibit MNNG-induced apoptosis in this cell type.

Discussion

Several recent reports showed that exposure of cells to the monofunctional alkylating agent MNNG can result in the triggering of programmed cell death (Hickman and Samson, 1999; Meikrantz et al., 1998; Ochs and Kaina, 2000; Yu et al., 2002). Ochs and Kaina (2000) established that the relative rate of MNNG-induced mutagenic O^6-methylguanine (O^6 MeG) adduct repair effected apoptotic onset in rodent (CHO) cells. For example, higher doses of MNNG or reduced expression of the repair protein methylguanine methyltransferase (MGMT) exerted a positive effect on the percentage of cells in apoptosis. Similar findings were reached by Meikrantz et al. (1998). Hence, as concluded by these groups and supported by this work, the O^6 MeG adduct produced by MNNG is a potent apoptosis-inducing DNA lesion.

While clearly capable of triggering cell death, the apoptogenic pathway(s) activated by MNNG are not well understood. In this study, we focused on further defining a role for p53 in triggering MNNG-induced apoptosis. Caution must be taken in analyzing cells with compromised p53 function primarily due to the well-characterized "guardian of the genome" function attributed to p53 (Lane, 1992). As a result, p53-deficient cells possess relaxed control over genome integrity and allow a more permissive setting for development of secondary mutagenic events. In this study, we have used both an established p53-mutant cell line (WTK-1) and a recently engineered p53-ablated (B310-E6) cell line. In virtually every test conducted, we found that these cells behaved in a parallel

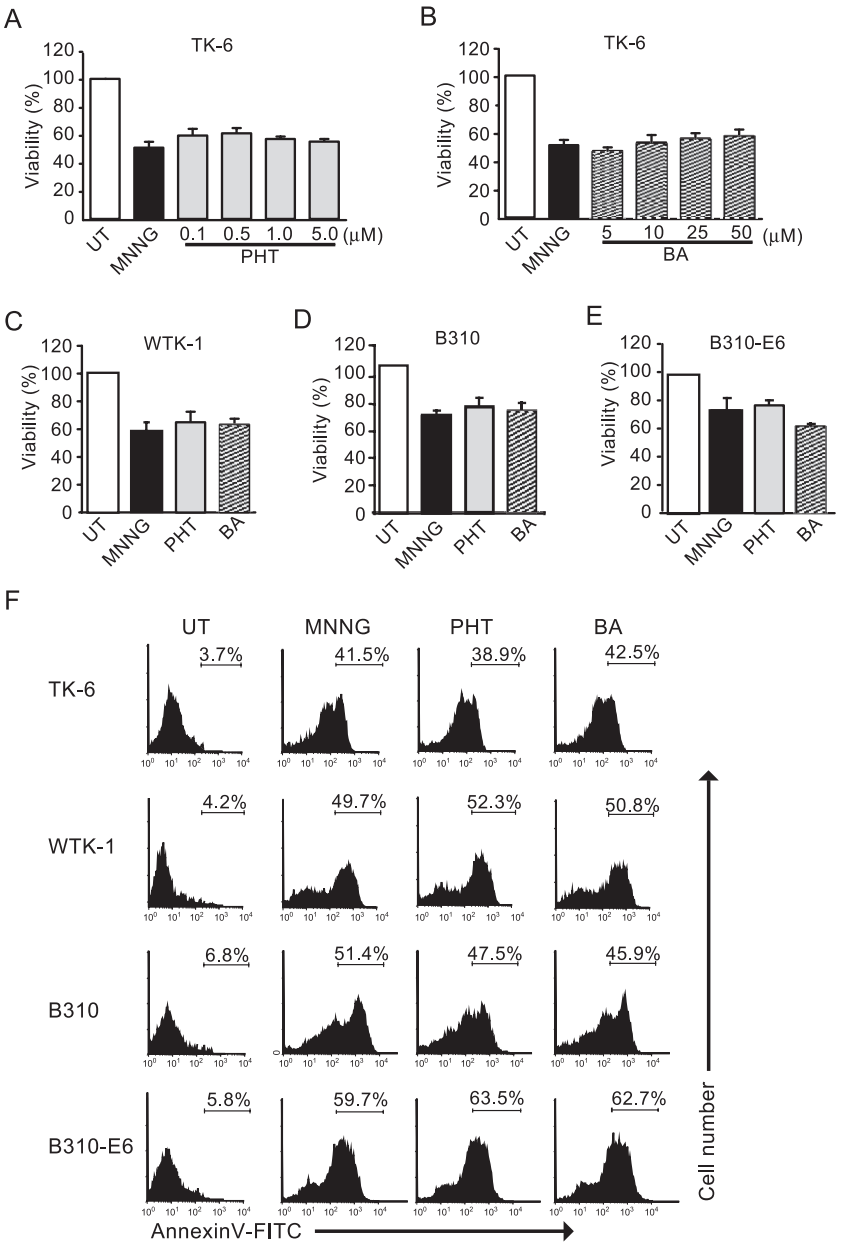

Fig. 8. Inhibition of PARP activity does not reduce MNNG-induced apoptotic onset in human lymphoblasts. (A) TK-6 cells were either untreated (open bar), treated with 15 μM MNNG only (filled bar), or treated with 15 μM MNNG in the presence of indicated concentrations of PHT (shaded bars). Following MNNG treatment (24 h), cell viability was quantified by MTS. (B) TK-6 cells were treated as in A but were incubated with the indicated concentration of BA (crosshatched bars). (C) WTK-1 cells were either untreated (open bar), treated with 15 μM MNNG only (filled bar), or treated with 15 μM MNNG in the presence of 5 μM PHT (shaded bar) or 50 μM BA (crosshatched bar). Following MNNG treatment (72 h), cell viability was quantified by MTS. (D) B310 cells were treated and analyzed as in C. (E) B310-E6 cells were treated and analyzed as in C. In all cases, graphed is the mean of at least three independent experiments, error bars = 1 SD. (F) Indicated human lymphoblastoid lines were either untreated, treated with 15 μM MNNG only, treated with 15 μM MNNG and 5 μM PHT, or 15 μM MNNG and 50 μM BA. Following a 24-h (TK-6 and B310) or 72-h incubation (WTK-1 and B310-E6), cells were processed for annexin V staining and analyzed by flow cytometry. Percentage of cells displaying positive annexin V staining is indicated.

manner when contrasted with related p53-proficient cells (TK-6 and B310, respectively). Thus, while we cannot strictly rule out that observed differences in apoptotic response between p53-proficient and deficient cells are not due to secondary mutations, the most straightforward conclusion based on our findings is that p53 is a component in MNNG-induced apoptogenic signaling.

Hickman and Samson (1999) observed that human lymphoblasts expressing the HPV E6 protein showed a delay in apoptotic entry suggesting a nonessential role for p53 in this process. In our study, we found that cells expressing mutant p53 (WTK-1) and ablated p53 (B310-E6) showed a kinetically slower rate of apoptotic onset than matched cells expressing wild-type p53. These results are consistent with

the activation of at least two apoptogenic pathways: One is rapid, robust, and dependent upon p53; the other pathway is triggered in a kinetically slower fashion, proceeds at a more deliberate pace and is triggered in a p53-independent fashion. Similar conclusions were drawn by others studying irradiated lymphoblasts (Yu and Little, 1998; Yu et al., 1997). While it is tempting to conclude that IR and MNNG may activate the same apoptogenic pathways, we are currently unsure if these two genotoxins, which cause structurally dissimilar types of DNA damage, trigger identical pro-death mechanisms.

We observed in human lymphoblastoid cells that p53-deficiency leads to reduced sensitivity to MNNG. This is reminiscent of the "alkylation tolerant" phenotype displayed by cells deficient in mismatch repair (MMR) (Aquilina et al., 1993; Branch et al., 1993; Goldmacher et al., 1986; Kat et al., 1993). More recently, Hickman and Samson (1999) found that the mismatch repair complex MutSα (MSH2/MSH6 heterodimer) was required for signaling the initiation of apoptosis in response to MNNG and, to a lesser extent, the nitrosourea BCNU. Our laboratory has recently shown that radiation-induced activation of the kinase Chk2 is dysregulated in MMR-deficient cells (Brown et al., 2003). Chk2 phosphorylates p53 in response to DNA damage (Hirao et al., 2000), and work from several labs (Hirao et al., 2002; Jack et al., 2002; Takai et al., 2002) indicates that Chk2 is required for irradiation-induced apoptosis in mice and cultured mouse cells. In contrast, recent reports from Jallepalli et al. (2003) and Ahn et al. (2003) showed that Chk2 was not required for p53-dependent response to ionizing radiation in human cells. Thus, at present, the role of Chk2 in activation of p53-dependent apoptosis is ambiguous. Nevertheless, in light of the phenotypic similarities in the apoptotic response to MNNG shown by both MMR and p53-deficient cells, it is feasible to speculate that these phenotypes stem from defects in the same apoptogenic mechanisms. Alternatively, pro-apoptotic activation of p73 requires MMR in response to cisplatin-induced damage (Gong et al., 1999); thus, it is plausible that, separately, MMR deficiency and p53 deficiency lead to similar phenotypes by inactivating distinct, yet parallel, apoptogenic mechanisms.

Our findings underscore a potential role for p53 in triggering apoptosis; however, we are currently unsure how p53 exerts control over MNNG-induced cell death. We have observed that both the p53-dependent and -independent pathways promote decreased mitochondrial transmembrane potential and accumulation of the mitochondrial protein cytochrome *c* within the cytosol. Expression of many of the members of the Bcl2 family are controlled by p53 and are capable of driving increases mitochondrial permeability. Furthermore, previous studies found that overexpression of Bcl2 in CHO cells blocked MNNG-induced apoptosis (Meikrantz et al., 1998; Ochs and Kaina, 2000) presumably by blocking decreases in mitochondrial transmembrane potential (Zamzami et al., 1998). Taken together, these findings clearly suggest that, in response to MNNG, p53 controls the expression of Bcl2-family members, and perhaps other proteins, resulting in increased mitochondrial permeability. Of note, we observed that activation of the p53-independent pathway also resulted in increased mitochondrial permeability. Zhan et al. (1997) reported that the Bcl2 family member Mcl1 can be upregulated in a p53-independent manner following DNA damage; thus, it is reasonable to speculate that a subset of proteins that drive increases in mitochondrial permeability during p53-dependent apoptosis may also be upregulated during MNNG-induced p53-independent apoptosis.

Caspases are a class of evolutionarily conserved cysteine proteases that play a crucial role in apoptotic mechanisms present in a variety of species. Current views hold that one of the functions of caspases, more specifically the effector caspases such as caspase-3, during programmed cell death is to inactivate vital cellular proteins such as structural proteins like lamins and gelsolin, DNA repair proteins (such as DNA-PKcs), and key signaling molecules like PKXδ (for review, see Nicholson and Thornberry, 1997). Paradoxically, some proteins acquire apoptosis-promoting properties following caspase-dependent cleavage such as PARP (Kim et al., 2000) and BRCA-1 (Zhan et al., 2002). We found that during both p53-dependent and -independent apoptosis that caspase-9 and -3 were activated. MNNG-induced activation of caspase-9 is consistent with our finding that this drug induced accumulation of cytosolic cytochrome *c* which, in turn, drives caspase-9 activation by promoting formation of the apoptosome (Shi, 2002). We observed that both zVAD-fmk and zDEVD-fmk inhibited caspase-3 activity in human lymphoblasts; however, these inhibitors we only able to effectuate a significant block of cell death in TK-6 cells measured 24 h after drug exposure. Further, while we measured no significant effects of z-VAD-fmk on MNNG-induced apoptosis in B310, we did observe that the caspase inhibitor z-DEVD-fmk was able to significantly block apoptosis in B310 cells at the same time after drug. At this early time point, apoptotic response in TK-6 and B-310 is chiefly attributable to the triggering of p53-dependent pathways. Thus, our finding that caspase inhibitors can partially block apoptosis in TK-6 cells seemingly indicates that rapid p53-dependent cell death activated by MNNG is more dependent upon caspase activity than are the slower p53-independent mechanisms triggered in WTK-1 and B310-E6 cells.

PARP catalyzes the ADP ribosylation of damaged DNA and this activity is though to play a critical role in DNA repair (for review, see Ziegler and Oei, 2001). PARP also plays a key role in triggering apoptosis. How PARP contributes to cell death in response to DNA damage remains debatable but several lines of evidence have recently shed light on this subject. First, PARP enzymatic activity uses β-nicotinamide adenine dinucleotide (NAD^+) as the substrate in a reaction that catabolizes NAD^+ into nicotinamide (NAD) and poly(-ADP-ribose). Based on this, it has been proposed that activation of PARP will exhaust the cell of NAD^+ and ATP,

leading to energy depletion and cell death (Lieberthal et al., 1998; Ran et al., 1999). Second, it has recently been shown that PARP is required for the translocation of AIF to the nucleus (Yu et al., 2002). Once in the nucleus, AIF binds to DNA and induces chromatin condensation and DNA fragmentation, and as a result of this activity, promotes cell death (Cande et al., 2002). We observed that two different PARP inhibitors (benzamide and PHT) used at concentrations that resulted in inhibition of PARP activity (as judged by diminished ADP-ribosylation of proteins in response to MNNG exposure) and significant blockage of AIF translocation to the nucleus failed to produce a significant effect on MNNG-induced cell death human lymphoblasts. This finding may suggest that PARP activity is not required for the p53-dependent and -independent apoptogenic pathways activated by MNNG in this cell type. Alternatively, it is plausible that the PARP inhibitor concentrations used in this study failed to fully block PARP function and that residual enzymatic activity remained sufficient to drive cell death. We attempted to address the latter of these possibilities but found that higher concentrations of BA or PHT were cytotoxic in this cell type (data not shown).

In conclusion, we have uncovered that the S_N1 alkylator MNNG activates both p53-dependent and -independent apoptogenic mechanisms and loss of p53 results in heightened tolerance to the cytotoxic effects of MNNG. The p53-dependent mechanism is rapid while the p53-independent mechanism is triggered in a kinetically slower fashion. Both mechanisms converge at the mitochondria and force decreases in mitochondrial transmembrane potential, release of cytochrome *c* into the cytosol, and activate caspase-9 and -3. Experiments using caspase inhibitors suggest that the rapid p53-dependent apoptotic pathway relies more heavily on caspase activity to kill cells than the slower p53-independent pathway. Conversely, inhibition of PARP activity had no detectable effect on MNNG-induced programmed cell death. These findings support the conclusion that MNNG activates multiple apoptogenic pathways that contain both common and unique mechanisms.

Acknowledgments

The authors thank Dr. John Little (Harvard School of Public Health) for his generous gift of TK-6 and WTK-1 cells, and Dr. Denise Galloway for PA-317 cells that package the E6-encoding retrovirus. This work was supported by grants from the American Cancer Society and NIH/NCI to KDB. AWA and DIB were supported, in part, by predoctoral fellowships from the Stanley S. Scott Cancer Center.

References

Adamson, A.W., Kim, W.J., Shangary, S., Baskaran, R., Brown, K.D., 2002. ATM is activated in response to MNNG-induced DNA alkylation. J. Biol. Chem. 31, 31.

Ahn, J., Urist, M., Prives, C., 2003. Questioning the role of checkpoint kinase 2 in the p53 DNA damage response. J. Biol. Chem. 278, 20480–20489.

Antonicka, H., Floryk, D., Klement, P., Stratilova, L., Hermanska, J., Houstkova, H., Kalous, M., Drahota, Z., Zeman, J., Houstek, J., 1999. Defective kinetics of cytochrome *c* oxidase and alteration of mitochondrial membrane potential in fibroblasts and cytoplasmic hybrid cells with the mutation for myoclonus epilepsy with ragged-red fibres ('MERRF') at position 8344 nt. Biochem. J. 342 (Pt 3), 537–544.

Aquilina, G., Biondo, R., Dogliotti, E., Bignami, M., 1993. Genetic consequences of tolerance to methylation DNA damage in mammalian cells. Carcinogenesis 14, 2097–2103.

Bauer, M.K., Schubert, A., Rocks, O., Grimm, S., 1999. Adenine nucleotide translocase-1, a component of the permeability transition pore, can dominantly induce apoptosis. J. Cell Biol. 147, 1493–1502.

Beardsley, D.I., Kowbel, D., Lataxes, T.A., Mannino, J.M., Xin, H., Kim, W.J., Collins, C., Brown, K.D., 2003. Characterization of the novel amplified in breast cancer-1 (NABC1) gene product. Exp. Cell Res. 290, 402–413.

Branch, P., Aquilina, G., Bignami, M., Karran, P., 1993. Defective mismatch binding and a mutator phenotype in cells tolerant to DNA damage. Nature 362, 652–654.

Brenner, C., Cadiou, H., Vieira, H.L., Zamzami, N., Marzo, I., Xie, Z., Leber, B., Andrews, D., Duclohier, H., Reed, J.C., Kroemer, G., 2000. Bcl-2 and Bax regulate the channel activity of the mitochondrial adenine nucleotide translocator. Oncogene 19, 329–336.

Brown, K.D., Ziv, Y., Sadandanan, S.N., Chessa, L., Collins, F.S., Shiloh, Y., Tagle, D.A., 1997. The ataxia-telangiectasia gene product, a constitutively expressed nuclear protein that is not upregulated following genome damage. Proc. Natl. Acad. Sci. 94, 1840–1845.

Brown, K.D., Rathi, A., Kamath, R., Beardsley, D.I., Zhan, Q., Mannino, J.L., Baskaran, R., 2003. The mismatch repair system is required for S-phase checkpoint activation. Nat. Genet. 33, 80–84.

Cande, C., Cecconi, F., Dessen, P., Kroemer, G., 2002. Apoptosis-inducing factor (AIF): key to the conserved caspase-independent pathways of cell death? J. Cell Sci. 115, 4727–4734.

Casciola-Rosen, L., Nicholson, D.W., Chong, T., Rowan, K.R., Thornberry, N.A., Miller, D.K., Rosen, A., 1996. Apopain/CPP32 cleaves proteins that are essential for cellular repair: a fundamental principle of apoptotic death. J. Exp. Med. 183, 1957–1964.

Chao, C., Saito, S., Kang, J., Anderson, C.W., Appella, E., Xu, Y., 2000. p53 transcriptional activity is essential for p53-dependent apoptosis following DNA damage. EMBO J. 19, 4967–4975.

el-Deiry, W.S., Tokino, T., Velculescu, V.E., Levy, D.B., Parsons, R., Trent, J.M., Lin, D., Mercer, W.E., Kinzler, K.W., Vogelstein, B., 1993. WAF1, a potential mediator of p53 tumor suppression. Cell 75, 817–825.

Goldmacher, V.S., Cuzick Jr., R.A., Thilly, W.G., 1986. Isolation and partial characterization of human cell mutants differing in sensitivity to killing and mutation by methylnitrosourea and *N*- methyl-*N*′-nitro-*N*-nitrosoguanidine. J. Biol. Chem. 261, 12462–12471.

Gong, J.G., Costanzo, A., Yang, H.Q., Melino, G., Kaelin Jr., W.G., Levrero, M., Wang, J.Y., 1999. The tyrosine kinase c-Abl regulates p73 in apoptotic response to cisplatin-induced DNA damage. Nature 399, 806–809.

Greenwood, S.K., Armstrong, M.J., Hill, R.B., Bradt, C.I., Johnson, T.E., Hilliard, C.A., Galloway, S.M., 1998. Fewer chromosome aberrations and earlier apoptosis induced by DNA synthesis inhibitors, a topoisomerase II inhibitor or alkylating agents in human cells with normal compared with mutant p53. Mutat. Res. 401, 39–53.

Halbert, C.L., Demers, G.W., Galloway, D.A., 1991. The E7 gene of human papillomavirus type 16 is sufficient for immortalization of human epithelial cells. J. Virol. 65, 473–478.

Hartwell, L., Weinert, T., Kadyk, L., Garvik, B., 1994. Cell cycle checkpoints, genomic integrity, and cancer. Cold Spring Harbor Symp. Quant. Biol. 59, 259–263.

Hickman, M.J., Samson, L.D., 1999. Role of DNA mismatch repair and p53 in signaling induction of apoptosis by alkylating agents. Proc. Natl. Acad. Sci. U.S.A. 96, 10764–10769.

Hickman, E.S., Moroni, M.C., Helin, K., 2002. The role of p53 and pRB in apoptosis and cancer. Curr. Opin. Genet. Dev. 12, 60–66.

Hirao, A., Kong, Y.Y., Matsuoka, S., Wakeham, A., Ruland, J., Yoshida, D., Liu, D., Elledge, S.J., Mak, T.W., 2000. DNA damage-induced activation of p53 by the checkpoint kinase Chk2. Science 287, 1824–1827.

Hirao, A., Cheung, A., Duncan, G., Girard, P.M., Elia, A.J., Wakeham, A., Okada, H., Sarkissian, T., Wong, J.A., Sakai, T., De Stanchina, E., Bristow, R.G., Suda, T., Lowe, S.W., Jeggo, P.A., Elledge, S.J., Mak, T.W., 2002. Chk2 is a tumor suppressor that regulates apoptosis in both an ataxia telangiectasia mutated (ATM)-dependent and an ATM-independent manner. Mol. Cell. Biol. 22, 6521–6532.

Jack, M.T., Woo, R.A., Hirao, A., Cheung, A., Mak, T.W., Lee, P.W., 2002. Chk2 is dispensable for p53-mediated G1 arrest but is required for a latent p53-mediated apoptotic response. Proc. Natl. Acad. Sci. U.S.A. 99, 9825–9829.

Jallepalli, P.V., Lengauer, C., Vogelstein, B., Bunz, F., 2003. The Chk2 tumor suppressor is not required for p53 responses in human cancer cells. J. Biol. Chem. 278, 20475–20479.

Karpinich, N.O., Tafani, M., Rothman, R.J., Russo, M.A., Farber, J.L., 2002. The course of etoposide-induced apoptosis from damage to DNA and p53 activation to mitochondrial release of cytochrome *c*. J. Biol. Chem. 277, 16547–16552.

Kat, A., Thilly, W.G., Fang, W.H., Longley, M.J., Li, G.M., Modrich, P., 1993. An alkylation-tolerant, mutator human cell line is deficient in strand- specific mismatch repair. Proc. Natl. Acad. Sci. U.S.A. 90, 6424–6428.

Kim, J.W., Kim, K., Kang, K., Joe, C.O., 2000. Inhibition of homodimerization of poly(ADP-ribose) polymerase by its C-terminal cleavage products produced during apoptosis. J. Biol. Chem. 275, 8121–8125.

Kroemer, G., Dallaporta, B., Resche-Rigon, M., 1998. The mitochondrial death/life regulator in apoptosis and necrosis. Annu. Rev. Physiol. 60, 619–642.

Li, C.Q., Trudel, L.J., Wogan, G.N., 2002. Nitric oxide-induced genotoxicity, mitochondrial damage, and apoptosis in human lymphoblastoid cells expressing wild-type and mutant p53. Proc. Natl. Acad. Sci. U.S.A. 99, 10364–10369.

Lane, D.P., 1992. Cancer. p53, guardian of the genome. Nature 358, 15–16.

Liber, H.L., Thilly, W.G., 1982. Mutation assay at the thymidine kinase locus in diploid human lymphoblasts. Mutat. Res. 94, 467–485.

Lieberthal, W., Menza, S.A., Levine, J.S., 1998. Graded ATP depletion can cause necrosis or apoptosis of cultured mouse proximal tubular cells. Am. J. Physiol. 274, F315–F327.

Marzo, I., Brenner, C., Zamzami, N., Jurgensmeier, J.M., Susin, S.A., Vieira, M.C., Prevost, M.C., Xie, Z., Matsuyama, S., Reed, J.C., Kroemer, G., 1998. Bax and adenine nucleotide translocator cooperate in the mitochondrial control of apoptosis. Science 281, 2027–2031.

Meikrantz, W., Bergom, M.A., Memisoglu, A., Samson, L., 1998. O6-alkylguanine DNA lesions trigger apoptosis. Carcinogenesis 19, 369–372.

Morris, S.M., Chen, J.J., Domon, O.E., McGarrity, L.J., Bishop, M.E., M.G., M.G., Manjanatha, M.G., Casciano, D.A., 1998. p53, mutations, and apoptosis in genistein-exposed human lymphoblastoid cells. Mutat. Res. 405, 41–56.

Nicholson, D.W., Thornberry, N.A., 1997. Caspases: killer proteases. Trends Biochem. Sci. 22, 299–306.

Ochs, K., Kaina, B., 2000. Apoptosis induced by DNA damage O6-methylguanine is Bcl-2 and caspase- 9/3 regulated and Fas/caspase-8 independent. Cancer Res. 60, 5815–5824.

Pan, G., Humke, E.W., Dixit, V.M., 1998a. Activation of caspases triggered by cytochrome *c* in vitro. FEBS Lett. 426, 151–154.

Pan, G., O'Rourke, K., Dixit, V.M., 1998b. Caspase-9, Bcl-XL, and Apaf-1 form a ternary complex. J. Biol. Chem. 273, 5841–5845.

Ran, Z., Rayet, B., Rommelaere, J., Faisst, S., 1999. Parvovirus H-1-induced cell death: influence of intracellular NAD consumption on the regulation of necrosis and apoptosis. Virus Res. 65, 161–174.

Rasola, A., Geuna, M., 2001. A flow cytometry assay simultaneously detects independent apoptotic parameters. Cytometry 45, 151–157.

Scheffner, M., Huibregtse, J.M., Vierstra, R.D., Howley, P.M., 1993. The HPV-16 E6 and E6-AP complex functions as a ubiquitin-protein ligase in the ubiquitination of p53. Cell 75, 495–505.

Shen, Y., White, E., 2001. p53-dependent apoptosis pathways. Adv. Cancer Res. 82, 55–84.

Shi, Y., 2002. Mechanisms of caspase activation and inhibition during apoptosis. Mol. Cell 9, 459–470.

Strasser, A., O'Connor, L., Dixit, V.M., 2000. Apoptosis signaling. Annu. Rev. Biochem. 69, 217–245.

Sun, X.M., MacFarlane, M., Zhuang, J., Wolf, B.B., Green, D.R., Cohen, G.M., 1999. Distinct caspase cascades are initiated in receptor-mediated and chemical-induced apoptosis. J. Biol. Chem. 274, 5053–5060.

Takai, H., Naka, K., Okada, Y., Watanabe, M., Harada, N., Saito, S., Anderson, C.W., Appella, E., Nakanishi, M., Suzuki, H., Nagashima, K., Sawa, H., Ikeda, K., Motoyama, N., 2002. Chk2-deficient mice exhibit radioresistance and defective p53-mediated transcription. EMBO J. 21, 5195–5205.

van Engeland, M., Nieland, L.J., Ramaekers, F.C., Schutte, B., Reutelingsperger, C.P., 1998. Annexin V-affinity assay: a review on an apoptosis detection system based on phosphatidylserine exposure. Cytometry 31, 1–9.

Virag, L., Szabo, C., 2002. The therapeutic potential of poly(ADP-ribose) polymerase inhibitors. Pharmacol. Rev. 54, 375–429.

Walker, L.S., McLeod, J.D., Boulougouris, G., Patel, Y.I., Ellwood, C.N., Hall, N.D., Sansom, D.M., 1999. Lack of activation induced cell death in human T blasts despite CD95L up-regulation: protection from apoptosis by MEK signalling. Immunology 98, 569–575.

Xia, F., Wang, X., Wang, Y.H., Tsang, N.M., Yandell, D.W., Kelsey, K.T., Liber, H.L., 1995. Altered p53 status correlates with differences in sensitivity to radiation-induced mutation and apoptosis in two closely related human lymphoblast lines. Cancer Res. 55, 12–15.

Yu, Y., Little, J.B., 1998. p53 is involved in but not required for ionizing radiation-induced caspase-3 activation and apoptosis in human lymphoblast cell lines. Cancer Res. 58, 4277–4281.

Yu, Y., Li, C.Y., Little, J.B., 1997. Abrogation of p53 function by HPV16 E6 gene delays apoptosis and enhances mutagenesis but does not alter radiosensitivity in TK6 human lymphoblast cells. Oncogene 14, 1661–1667.

Yu, S.W., Wang, H., Poitras, M.F., Coombs, C., Bowers, W.J., Federoff, H.J., Poirier, G.G., Dawson, T.M., Dawson, V.L., 2002. Mediation of poly(ADP-ribose) polymerase-1-dependent cell death by apoptosis-inducing factor. Science 297, 259–263.

Zamzami, N., Brenner, C., Marzo, I., Susin, S.A., Kroemer, G., 1998. Subcellular and submitochondrial mode of action of Bcl-2-like oncoproteins. Oncogene 16, 2265–2282.

Zamzami, N., El Hamel, C., Maisse, C., Brenner, C., Munoz-Pinedo, C., Belzacq, A.S., Costantini, P., Vieira, H., Loeffler, M., Molle, G., Kroemer, G., 2000. Bid acts on the permeability transition pore complex to induce apoptosis. Oncogene 19, 6342–6350.

Zhan, Q., Bieszczad, C.K., Bae, I., Fornace Jr., A.J., Craig, R.W., 1997. Induction of BCL2 family member MCL1 as an early response to DNA damage. Oncogene 14, 1031–1039.

Zhan, Q., Jin, S., Ng, B., Plisket, J., Shangary, S., Rathi, A., Brown, K.D., Baskaran, R., 2002. Caspase-3 mediated cleavage of BRCA1 during UV-induced apoptosis. Oncogene 21, 5335–5345.

Ziegler, M., Oei, S.L., 2001. A cellular survival switch: poly(ADP-ribosyl)ation stimulates DNA repair and silences transcription. Bioessays 23, 543–548.